Calibrating Wiedemann-99 Model Parameters to Trajectory Data of Mixed Vehicular Traffic

Ankit Anil Chaudhari

Former M. Tech student, Transportation Engineering

Department of Civil Engineering

Indian Institute of Technology, Madras. India 600036

Email: ankit9496@gmail.com

Dr. Karthik K. Srinivasan*

Professor

Department of Civil Engineering

Indian Institute of Technology, Madras. India 600036

Email: karthikks@iitm.ac.in

Dr. Bhargava Rama Chilukuri

Assistant Professor

Department of Civil Engineering

Indian Institute of Technology, Madras. India 600036

Email: bhargava@iitm.ac.in

Dr. rer. nat. Martin Treiber

Institute of Transport and Economics

Faculty of Transport and Traffic sciences

Technische Universität Dresden, Dresden, Germany. 01062

Email: martin.treiber@tu-dresden.de

Dr. rer. pol. Ostap Okhrin

Professor

Chair of Econometric and Statistics esp. in the Transport sector

Institute of Transport and Economics

Faculty of Transport and Traffic sciences

Technische Universität Dresden, Dresden, Germany. 01062

Email: ostap.okhrin@tu-dresden.de

Word Count: 7796 words + 1 Table (250 words) = 8046

Submitted [1 February 2020]

*Corresponding Author

ABSTRACT

We propose a new methodology for calibrating Wiedemann-99 vehicle-following parameters for mixed traffic (different conventional vehicle classes) based on trajectory data. The existing acceleration equations of the Wiedemann model are modified to represent more realistic driving behavior. Exploratory analysis of simulation data revealed that different Wiedemann-99 model parameters could lead to similar macroscopic behavior, highlighting the importance of calibration at the microscopic level. Therefore, the proposed methodology is based on optimizing performance measures at the microscopic level (acceleration, speed, and trajectory profiles) to estimate suitable calibration parameters. Further, the goodness of fit for the observed data is sensitive to the numerical integration method used to compute vehicles' velocity and position. We found that the calibrated parameters using the proposed methodology perform better than other approaches for calibrating mixed traffic. The results reveal that the calibrated parameter values and, consequently, the thresholds that delineate closing, following, emergency braking, and opening regimes, vary between two-wheelers and cars. The window (in the relative speed vs. gap plot) for the unconscious following is larger for cars while the free flow regime is more extensive for two-wheelers. Moreover, under the same relative speed and gap stimulus, two-wheelers and cars may be in different regimes and display different acceleration responses. Thus, accurate calibration of each vehicle's parameters is essential for developing micro-simulation models for mixed traffic. The calibration analysis results of strict and overlapping staggered car-following signify an impact of staggered car-following compared to strict car-following which demands separate calibration for strict and staggered following.

Keywords: "mixed traffic", "Wiedemann-99 model", "VISSIM", "microscopic calibration", "trajectory data".

1. INTRODUCTION

Microscopic traffic flow models represent traffic in greater detail and generate more performance measures than macroscopic or mesoscopic models. They enable evaluating a wide range of traffic interventions and scenarios prior to their implementation. Moreover, they reflect the dynamic and random nature of the transportation system (*1*). Therefore, they are robust and cost-efficient tools for modeling them.

A microscopic traffic flow model consists of sub-models that describe human driver behavior such as gap-acceptance, speed adaptation, lane-changing, ramp merging, overtaking, and car-following. The latter, on which we focus here, describes the interactions with preceding vehicles in the same lane including the special case of free flow with no interactions (*2*).

One of the critical elements of using microscopic models is calibration. The value of the simulation models' various parameters is determined to match the observed real traffic behavior. As no single traffic model can represent all the traffic conditions, every model must be adapted to local needs using real-world data. Hence, parameter calibration in simulation applications is critical to replicate field driving behavior. This study focuses on calibrating a widely-used psychophysical vehicle-following model (Wiedemann-99 (W-99) model) for India's mixed traffic conditions using vehicle trajectory data.

The W-99 (*3*) model has been widely used in traffic microsimulation for both lane-based and non-lane-based conditions (*1*, *4–12*). However, this model's use in non-lane-based states will be substantially different from lane-based conditions and requires careful calibration. These differences arise, in particular, from the presence and composition of additional vehicle types such as (two-wheelers or auto-rickshaws, different static and dynamic characteristics of vehicles, and a lack of strict lane discipline. As a result, vehicles are free to occupy any available lateral position on the road space. Moreover, smaller vehicles (two-wheelers) often utilize gaps between larger vehicles in the traffic stream (*13*). Another critical aspect of the non-lane-based mixed traffic condition is the possible difference in the following behavior when the subject vehicle is strictly behind a leading vehicle versus when it is overlapping and staggered compared to the vehicle ahead (*14*).

A recently proposed model for lane-free mixed traffic (*15*) provides a generalized framework for extending conventional car-following models (including the Wiedemann car-following model) to a fully two-dimensional microscopic model. In the presence of multiple leaders and staggered following, this framework assumes, with good results, that the longitudinal dynamics depends on the leader with the strongest interaction, only, and that the repulsive force remains unchanged as long as there is a lateral overlap, i.e., the longitudinal acceleration reverts to that of the underlying car-following model. One goal of the present analysis is to test this assumption by distinguishing between the strict and staggered following.

The key feature for calibration of mixed traffic conditions is the response of the driver of a subject vehicle to the vehicles present in the neighborhood and their maneuvers. One should note that the model parameters may vary based on leader, follower, and surrounding vehicle types and their speeds and positions (*16*). There is a growing body of work on the calibration of various microscopic models for mixed traffic using multiple models (*5*, *6*, *8–13*, *16–20*). The analytical forms of some of the Wiedemann model equations are not easily accessible in the literature, making the calibration at the trajectory level difficult. As a result, very few of these studies attempted to analyze the errors entailed in the calibration process of a Wiedemann model and its impacts on the accuracy of results at the trajectory level (*21*).

In light of the above motivations and gaps in the literature, this paper investigates the following objectives.

- Propose and implement an optimization-based procedure for calibrating the W-99 model vehicle-following parameters using trajectory data of mixed traffic
- Propose modifications of the acceleration equations to represent more realistic driving behavior.
- Evaluate alternative numerical integration methods for prediction of speed and position at the trajectory level
- Evaluate the proposed calibration with other calibration methods reported in the literature
- Analyze differences in the vehicle-following behavior of two-wheelers and cars in mixed traffic.
- Investigate differences in parameters between 'strict' and 'overlapping' following situations for selected vehicle types

The paper is organized as follows. Section 2 provides a brief review of the W-99 model and a synthesis of the literature with this study's objectives. The rationale for calibration of the W-99 model using trajectory data is presented in Section 3. In Section 4, we describe the data, and in Section 5 the calibration methodology. The salient results and findings are discussed in Section 6, followed by a few concluding remarks in Section 7.

2. LITERATURE REVIEW

The W-99 model is first presented in Section 2.1, followed by a synthesis of the literature on the calibration of car-following models in Section 2.2.

2.1 Wiedemann Car-Following Model

As a psychophysical model, the W-99 model (*3*) uses thresholds or action points, where the driver changes his/her behavior at discrete time points. Drivers change their response to the local situation (gap, speed, or relative speed) only when these thresholds are reached (*2*). This model's concept is that the faster moving drivers approaching slower vehicles start decelerating when they reach their perception threshold. However, due to imperfections in estimating speeds, the speed may become smaller than that of the leader. So, the driver may accelerate slightly again after reaching another threshold (*7*). The combined effect of the thresholds and estimation errors leads to a hysteresis when plotting the trajectory in the space given by the relative speed and the gap. Wiedemann (*22*) defined the relative speed between the lead and following vehicles as the stimulus, which triggers the following vehicle's reaction. Using different perception thresholds, four different driving regimes were proposed.

In the **free-flow regime,** the subject vehicle is not influenced by any other leader; the driver tries to maintain the desired speed and uses a speed-dependent maximum acceleration to reach the desired speed.

In the **closing-in regime,** the driver has perceived a slower leader and continuously decelerates till the speed matches the leader's speed (the relative speed becomes *zero*), and the gap equals the desired gap. Then, the driver enters the following regime.

In the **following regime,** the driver of the subject vehicle unconsciously follows the leader trying to maintain an ideal gap and zero relative speed using comparatively low accelerations or decelerations.

In the **emergency braking regime,** if the following distance falls below a critical threshold, the driver reacts by applying the maximum deceleration (within vehicular capabilities) to avoid a potential collision.

Figure 1 shows the boundaries of these regimes, which are defined by following six different perceptual thresholds:

- AX: the desired distance between two vehicles in a stopped condition,
- ABX: the desired minimum safe following distance in moving state, as a lower limit of the following regime,
- SDX: the maximum following distance as the upper limit of the following regime,
- SDV: the points at long distances (more than SDX) where drivers perceive that they are approaching slower vehicles,
- CLDV: the points at short distances (less than SDX) where drivers perceive that their speeds are higher than their lead vehicle speeds and
- OPDV: the points at short distances (less than SDX) where drivers perceive that they are traveling slower than their leader.

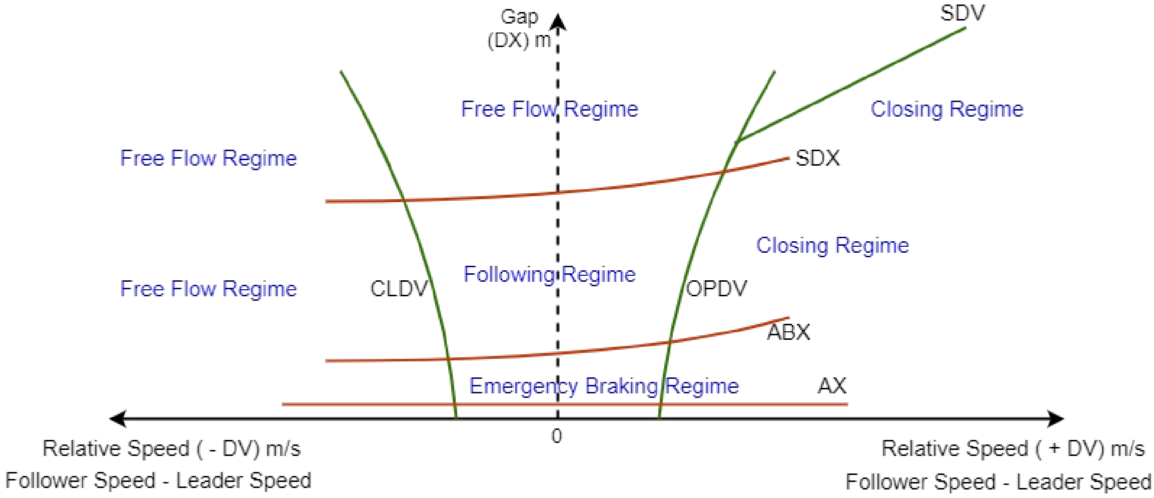

Figure 1 Schematic representation of Wiedemann Model (*22*)

The W-99 model (*3*) is calibrated using the driving behavior parameters (CC parameters); these parameters are defined based on regime classification thresholds. The description and the default value of CC parameters are given in Table 1.

Table 1: Wiedemann-99 parameters (*1*, *4*, *7*)

Parameters	**Description**	**Default Value**(*1*)
CCO	The desired gap between two vehicles in a stopped condition	**1.5 m**
CC1	Time gap following the driver keeps in for a safety in moving state	**0.9 s**
CC2	Range of gap between vehicles in the following regime	**4 m**
CC3	The time between the beginning of deceleration after perceiving of slow-moving leader to start the unconscious-following behavior	**-8 s**
CC4	Speed difference during the following process. CC4 controls speed differences during the opening process (Negative relative speed),	**-0.35 m/s**
CC5	Speed difference during the following process. CC5 controls speed differences in the closing process (Positive relative speed).	**0.35 m/s**
CC6	Influence of distance on speed oscillation during the following condition	**11.44 $(ms)^{-1}$**

CC7	Actual acceleration during oscillation in the unconscious-following regime	**0.25 m/s²**
CC8	Desired acceleration when the vehicle starting from the standing condition and	**3.5 m/s²**
CC9	Desired acceleration at 80km/hr. However, it is limited by maximum acceleration for the vehicle type.	**1.5 m/s²**

2.2 Calibration of Wiedemann Car-following Models in Heterogeneous Traffic

Many studies (*1*, *4*, *7*, *23*) have calibrated the Wiedemann parameters for homogeneous traffic flow data. Some of them have calibrated a single parameter set for all vehicle classes. In most studies (*8*–*12*, *17*, *18*) calibration procedures are based on matching the macroscopic performance measures from a simulation package (e.g., VISSIM) such as flow, density, speed, or delays with field data, primarily due to data limitations of cross-sectional video measurements. Other studies (*24*–*26*) used test track data or synthetic data for calibration of the vehicle-following models, and hence the applicability of the parameters to real-world traffic is unclear.

While trajectory data have been used to calibrate other vehicles following models such as the Gipps model (*27*) or the IDM (*28*), presumably due to the more straightforward equations involved, very few studies (*23*) focus on calibrating Wiedemann car-following models using trajectory data based on microscopic performance measures such as speed profiles of individual vehicles. This lack of studies is attributable partly due to limitations of data collected using location-based sensors, which give measurements at only selected cross-sections.

About mixed traffic, a growing number of studies have investigated the calibration of various vehicle-following models such as Krauss (*29*), Gipps (*27*), IDM (*28*), and W-99 (*3*). Again, the majority are based on macroscopic measures of performance. The mixed traffic flow model (MTM) is proposed as a generalized framework for car-following (*15*). A few other studies (*13*, *16*, *19*, *20*) aim to calibrate other models, such as Gipps's model and the IDM using field data. Still, they do not explicitly capture the differences in driving behaviors across regimes (following, closing. Emergency braking, opening, and free flow) sufficiently. Very few studies (*6*, *7*) have used microscopic trajectory data for calibrating W-99 models in mixed traffic but use heuristic or data-driven procedures to estimate vehicle-following parameters. Two essential concerns with these procedures include: the parameter estimates are not directly linked to differences between observed and computed trajectories at the microscopic level (position, speed, acceleration profiles of individual vehicles over time), and the quality of the resulting parameters is difficult to assess. Thus, there is a need for using optimization-based procedures to calibrate psychophysical models for mixed traffic using trajectory data. This will enable evaluating the effect of the model parameters on the deviation between observed vs. estimated speed, acceleration, and position profiles. Furthermore, in the context of mixed traffic, there is a need to understand whether, and to what extent, the W-99 parameters vary with the vehicle type (two-wheelers, cars, etc.) Another question is whether the parameter values found by trajectory calibration are comparable to those found with macroscopic calibration Finally, the influence of the kind of following (strict and staggered), specifically regime thresholds, also needs investigation in the context of the W-99 model.

In light of the above gaps, this study focuses on the W-99 car-following model's calibration using real-world trajectory data under heterogeneous and non-lane-based (mixed traffic) conditions. In this study, the W-99 model's acceleration equations are used for trajectory estimation rather than VISSIM generated data. W-99 parameters are calibrated by microscopic criteria such as the deviation between observed vs. estimated speed, acceleration, and position profiles at a microscopic level in mixed traffic data.

3. RATIONALE FOR CALIBRATING W-99 MODEL USING TRAJECTORY DATA

This section analyses the effect of different sets of microscopic vehicle-following parameters for mixed traffic on the resulting macroscopic traffic flow performance measures (average speed, flow, densities).

A study stretch (245 m) from a three-lane midblock section (described in Section 4) is considered for this analysis. Three different sets of the calibrated parameters values are input into the VISSIM traffic simulation software and macroscopic and microscopic measures (vehicle level position, speed, and acceleration profiles) are obtained for each set. Parameter sets 1, 2, and 3 (cf. Figure 2) are obtained by applying heuristics based on macroscopic criteria as reported in the literatures (*6*, *7*, *30*). The vehicular composition and vehicle dimensions (average length and width of each vehicle class) are taken from Kanagaraj et al. (*31*). Kinematic parameters (Maximum acceleration/deceleration, desired acceleration/deceleration, free-flow speed) are taken from Arasan and Koshy (*32*), Asaithambi et al. (*17*), and Kashyap et al. *(14)*. The differences in the CC parameters and associated threshold values across the sets are depicted in Figure 2 (for a constant leader speed of 10 m/s).

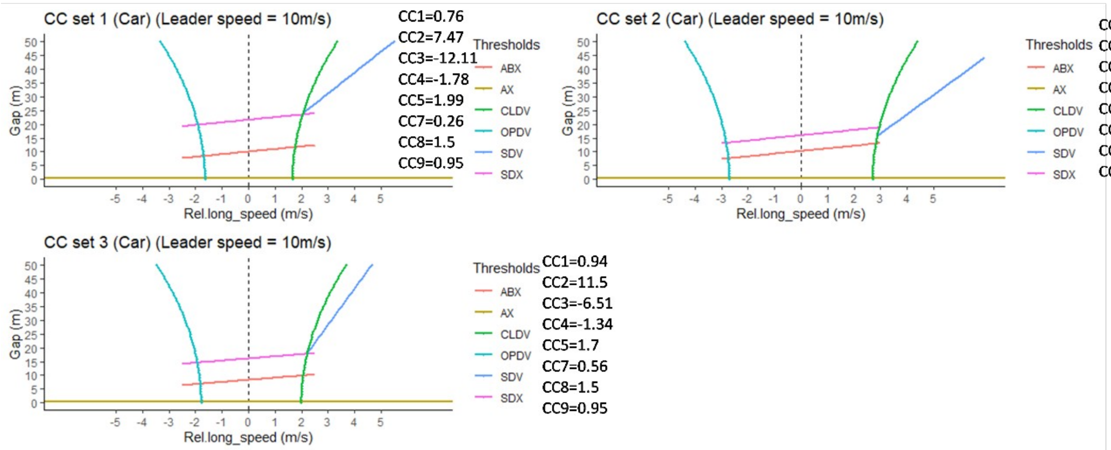

Figure 2. Wiedemann thresholds plots for different CC parameters

Table 2: Kinematic Parameters of Mixed Traffic Flow

Vehicle class	TW	Car	Bus	LCV	3W
Maximum Acceleration (m/s^2)	2.5	2.1	1.4	1.4	1.1
Desired Acceleration (m/s^2)	1.35	1.5	0.89	0.89	1.01
Maximum Deceleration (m/s^2)	-4.8	-4.2	-4	-4	-3.8

Desired Deceleration (m/s^2)	-4	-3.2	-2.8	-2.8	-3.4
Free Flow Speed (m/s)	13.8	13.6	12.5	12.5	11.5

The simulation model is run for a study period of 30 minutes for 100 different random seeds for a given set of Wiedemann parameters. The volume, density, and average speed for each vehicle class are calculated, and the procedure is repeated for different sets of Wiedemann parameters.

A set of pair-wise *t*-tests are performed for equal means of speed and density. In all sets, the equality of mean speed cannot be rejected (p-values were 0.2, 0.36, and 0.16 for CC set 1 and CC set 2, CC set 1 and CC set 3, CC set 2 and CC set 3, respectively). The mean densities are also not significantly different across the parameter sets (p-values were 0.58, 0.54, and 0.34, respectively, for the above pairs). Thus, the different cc parameter sets yield statistically similar macroscopic performance measures, despite the significant difference in microscopic behavior.

Trajectories of simulated data generated using the same input volume, speed, and acceleration distributions as explained above with the same random seed and different W-99 parameters (CC Sets 1, 2, and 3) are plotted in Figure 3. These trajectories are for the same single lane and for the same time interval for all sets of W-99 parameters. The macroscopic measures such as average speed, density, and volume of 100 replications of each set of CC parameters for three lanes study stretch (described in Section 4) are noted in the following plot. Major differences in the trajectories at the same time across different CC sets are marked with circles A, B, and C.

From left-hand circles (A) of each trajectory plot, we can see that,

1A – Trajectories are close to each other
2A- Trajectories are very scattered than 1A and 3A.
3A – There is a difference in the slope of some trajectories also some vehicles with some delay at the start.

From Central circles (B) of each trajectory plot, we can see that,

1B – Trajectories are very close to each other and some vehicles are crossing trajectories of other vehicles
2B – Vehicles in the circle have varied speed, some vehicle is showing delay at time 750.
3B – Vehicles are scattered as compared to 1B and 2B.

From the Right-Hand side circles (C) of each trajectory plot, we can see that,

1C – Most vehicles are moving at the same speed as trajectories are parallel, some vehicles are crossing trajectories of other vehicles
2C – Vehicles are very close to each other for time 810 to 820 and there is some lag in a vehicle starting at time 820
3C – Vehicles are close to each other than 1C but less close than 2C and lagged behavior of vehicles started at 820 is different from 2C.

These results indicate that different CC parameters show significantly different microscopic behavior but result in similar macroscopic behavior. Therefore, CC parameters need to be calibrated at a microscopic level to have consistency at that level.

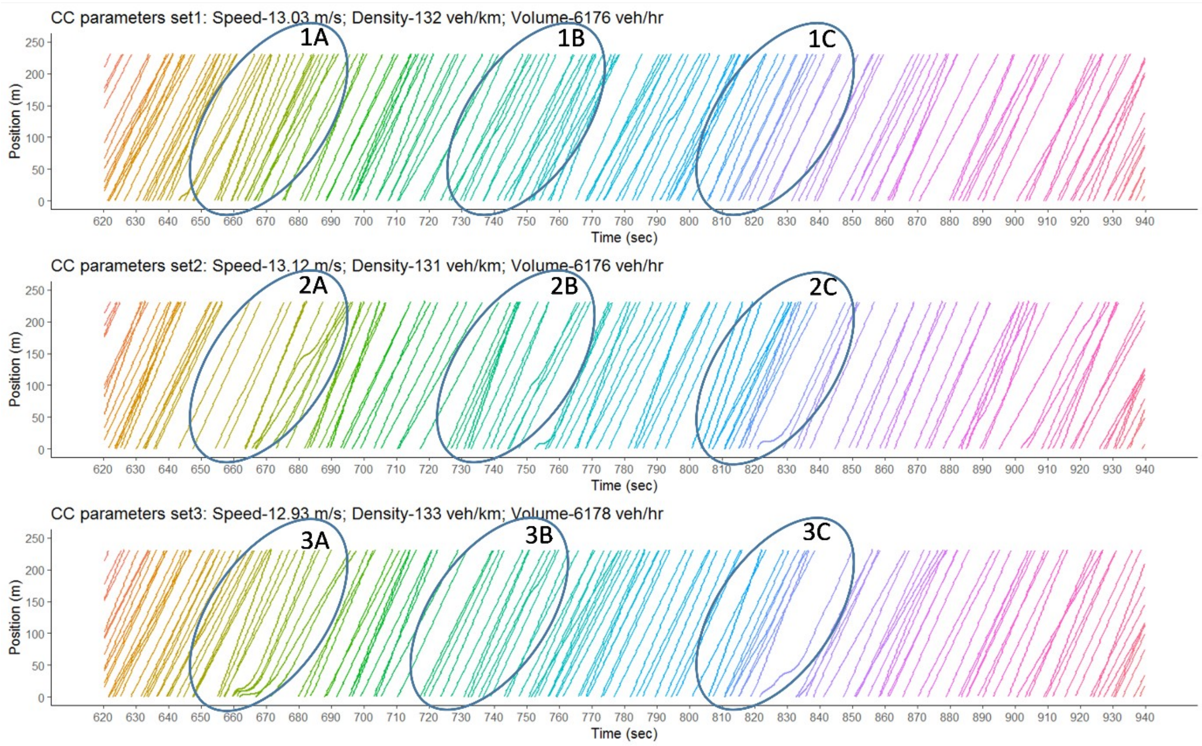

Figure 3. Trajectory Plots of Simulated Data for different sets of CC parameters

4. DATA COLLECTION

Video data were collected from a six-lane divided urban arterial road at the Maraimalai Adigalar Bridge in Saidapet, Chennai, India by Kanagaraj et al. (*31*). The selected section (Figure 4) is a bridge with a uniform road width. There are no nearby intersections, bus stops, parked vehicles, and other side friction that may affect drivers' behavior. Furthermore, there is no interaction between the vehicle traffic and pedestrians; the study section's width is 11.2m, and the length of the study section is 245m.

Figure 4. Snapshot of study section (*31*)

The coordinates, dimensions, and class of all vehicles in the video sequences for 30 minutes between 2:45 PM and 3:15 PM were obtained using a trajectory extractor. Data consists of a total of 3016 vehicles of 6 different classes. Data were recorded at a resolution of 0.52 s. (*31*)

4.1 Descriptive Statistics of Data

Traffic data consists of 1703 (57%) motorised two-wheelers (TW), 802 (27%) Car, 367 (12%) auto/three-wheelers, 95 (3%) Bus, 40 (1%) Light Commercial Vehicles (LCV) and 9 (0.29%) Heavy Commercial Vehicles (HCV). The collected dataset includes 3016 vehicle trajectories with a total of 130137 data points.

For the given data, vehicular trajectories are drawn as time-space plots. Figure 5 shows sample 82 trajectories of cars and 171 trajectories of two-wheelers for the same period. The vehicle trajectories have different slopes reflecting different speeds. Intersecting trajectories denote passing on either side. From both plots, we can see that there is different behavior of both vehicle classes; there is much variation in TW trajectories' slopes while that of the cars are comparatively steady. Furthermore, TWs have other values for the desired speed, the accelerations, and the longitudinal gaps (Section 3). Hence, TWs and cars have distinctively different longitudinal behavior.

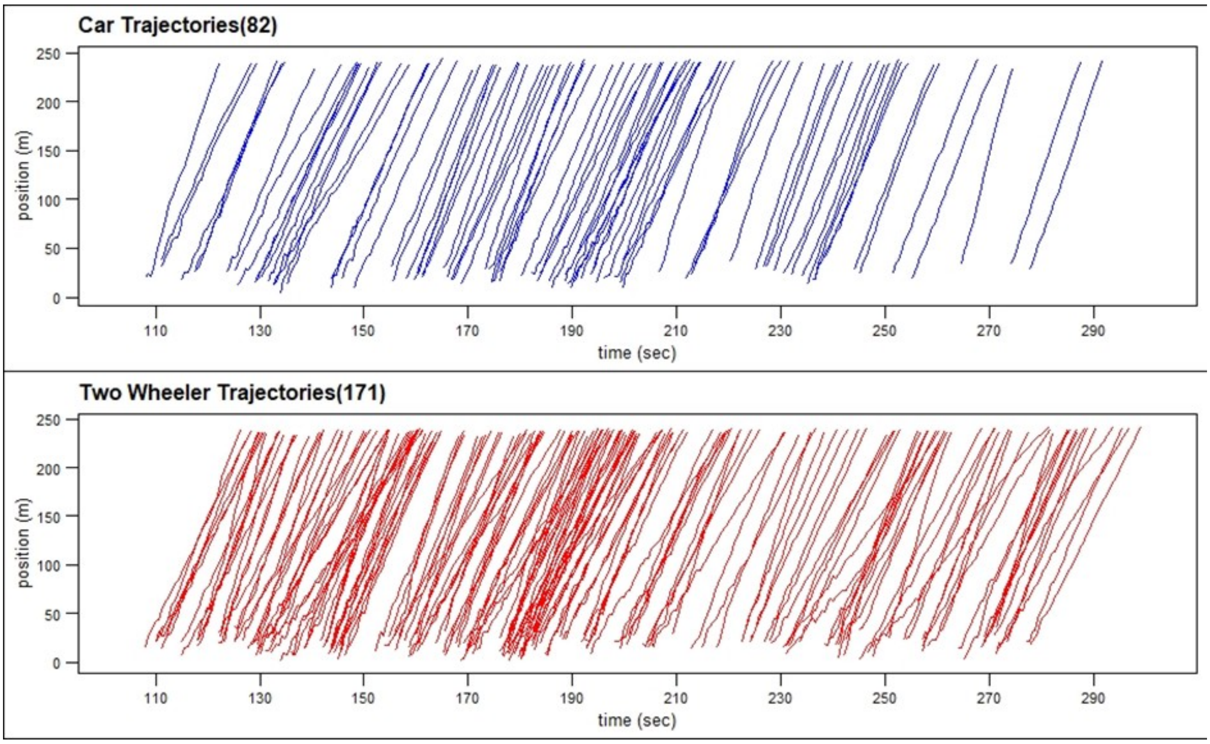

Figure 5. Trajectories Plot

4.2 Leader-Follower Pair Identification

The influence area method by Anand et al. (*16*) is selected for identifying the tentative leader-follower pairs. Using this method, a total of 2130 pairs are identified consisting of (TW:1056, Car:695, 3W:280, Bus:62, LCV:37) as subject vehicles.

Two features are essential in defining the following behavior. First, the follower can perceive the changes in the leader's speed/acceleration or gap when the leading vehicle is within certain limits and responds by changing his acceleration, speed, and position. Second, the following behavior must continue for a sufficient time duration.

Accordingly, the ‘actual’ or ‘true’ leader-follower pairs are identified based on the following criteria. The maximum longitudinal gap should be less than 30 m. No other vehicle should be present between an identified leader and follower. There must be lateral overlap between leader and follower. The following behavior (above three criteria) must be present for a duration greater than 5 seconds.

Pairs must show the hysteresis behavior i.e oscillations of relative speed and the gap from the unconscious following behavior as defined in the Wiedemann model to capture responsiveness of the follower to lead vehicle, sample hysteresis plots of relative speed (X-axis) and gap (Y-axis) are shown in Figure 6. The vehicle pair on Figure 6 (a) exhibits symmetric oscillations or hysteresis around the X-axis, in this regime, the follower tries to keep the same speed as the leader i.e. a relative speed near to zero, but the speed may become lesser/higher than that of the lead vehicle speed as a result of the driver’s imperfection in the estimation of the lead vehicle speed. So, the driver will accelerate/decelerate slightly again after reaching another threshold. This results in an iterative process of acceleration and deceleration leading to hysteresis due to drivers’ imperfections to determine the exact speeds of the leader; hence relative speed oscillates near zero, which is shown in the hysteresis plot Figure 6(a).

In contrast, as shown in Figure 6 (b) non-hysteresis behavior, there are no oscillations of the relative speed around zero in the following regime.

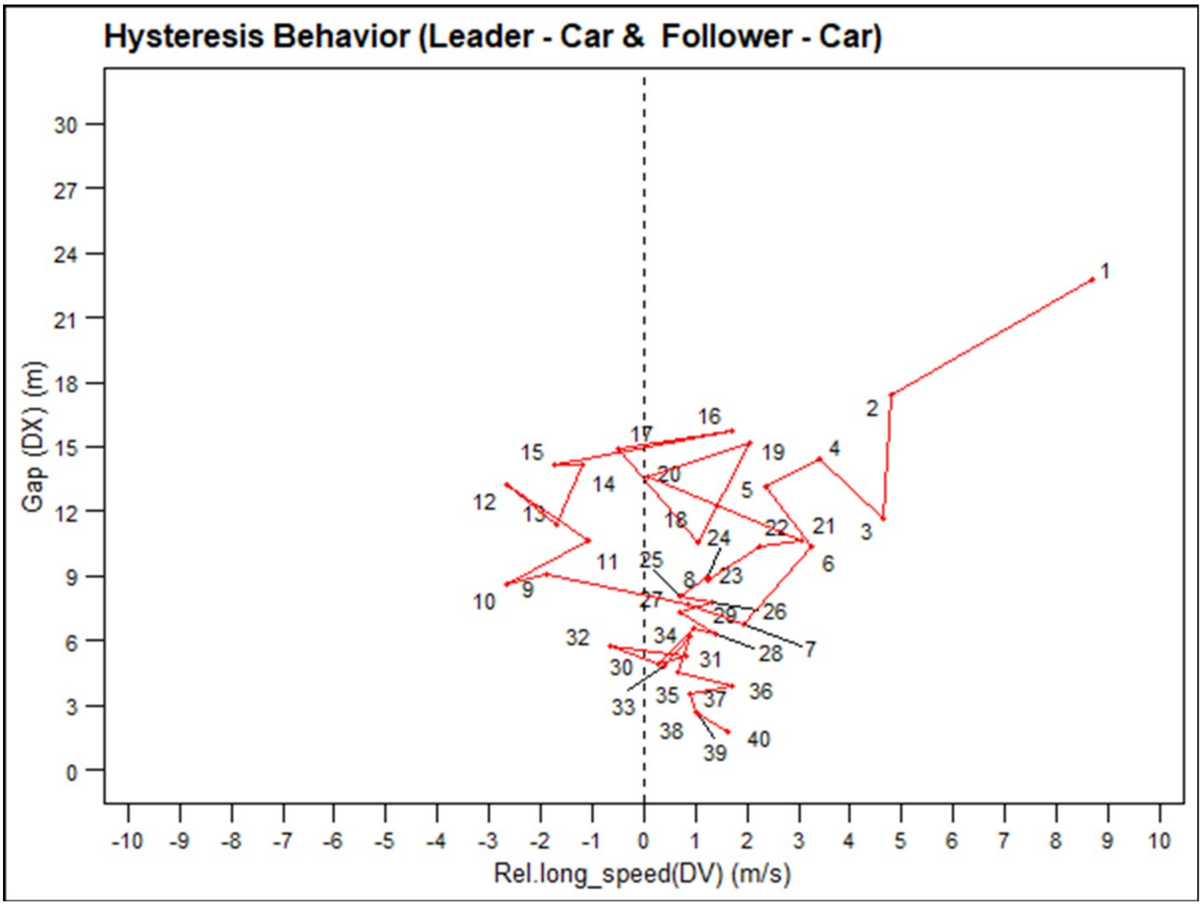

Figure 6 (a) Gap-Relative speed plot displaying hysteresis behavior

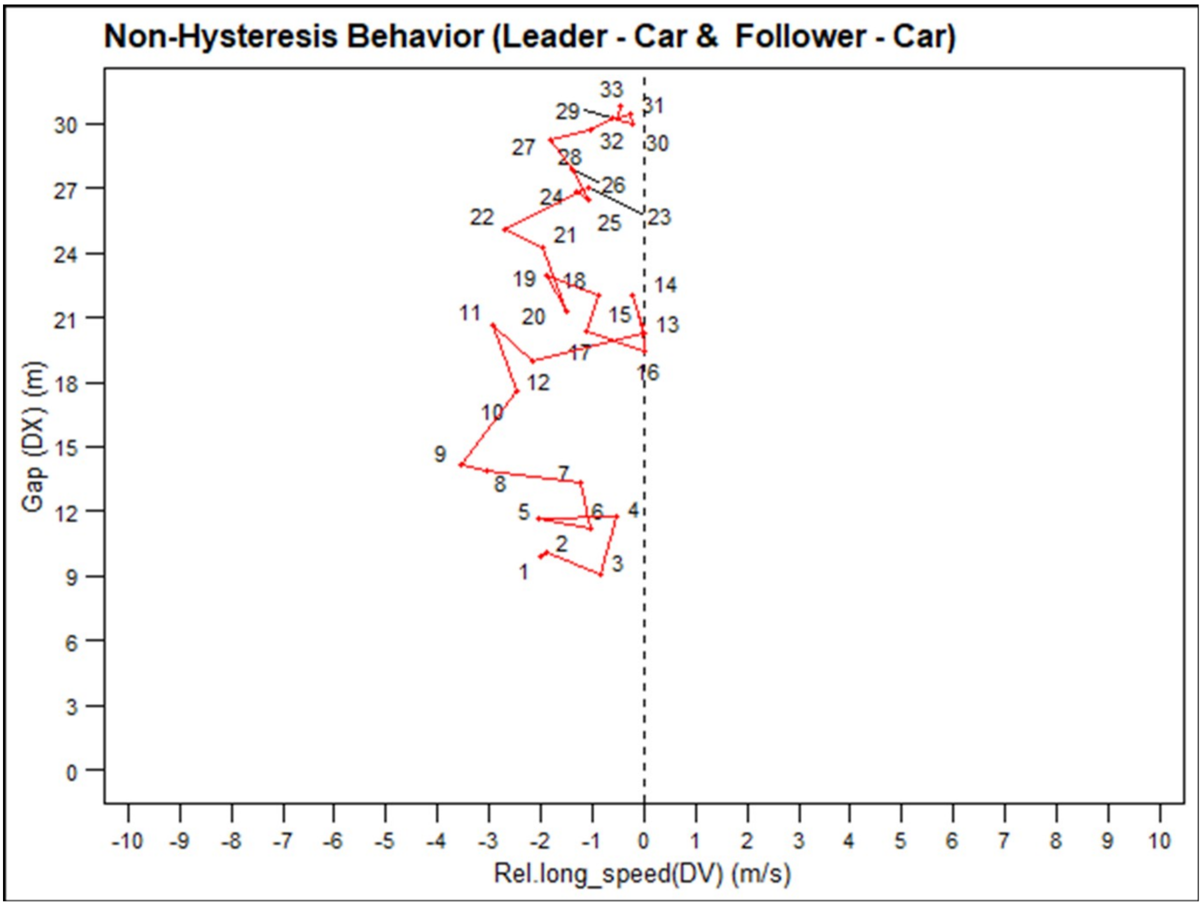

Figure 6 (b) Gap-Relative speed plot displaying non-hysteresis behavior

After applying the above conditions to the 2130 tentative leader-follower pairs, a total of 1236 (TW:544, Car:480, 3W:155, Bus:35, LCV:22) pairs are identified as true leader-follower pairs. Among these, very few cases with multiple leaders are identified (63 pairs out of 1024 pairs). For the calibration and analysis, subsequently, multiple leaders are considered as separate leaders. The following response can be taken as the most conservative response of the subject vehicle to these leaders. For all the regimes in multiple leaders' cases, a conservative braking approach is considered; i.e., for a data point, the smallest of predicted acceleration by all leaders is considered.

5. PROPOSED SCHEME FOR CALIBRATING W-99 PARAMETERS USING TRAJECTORY DATA IN MIXED TRAFFIC

This section explains the optimization-based procedure for calibrating W-99 following parameters using vehicle trajectory data in mixed traffic. Figure 7 gives an overview of the calibration methodology.

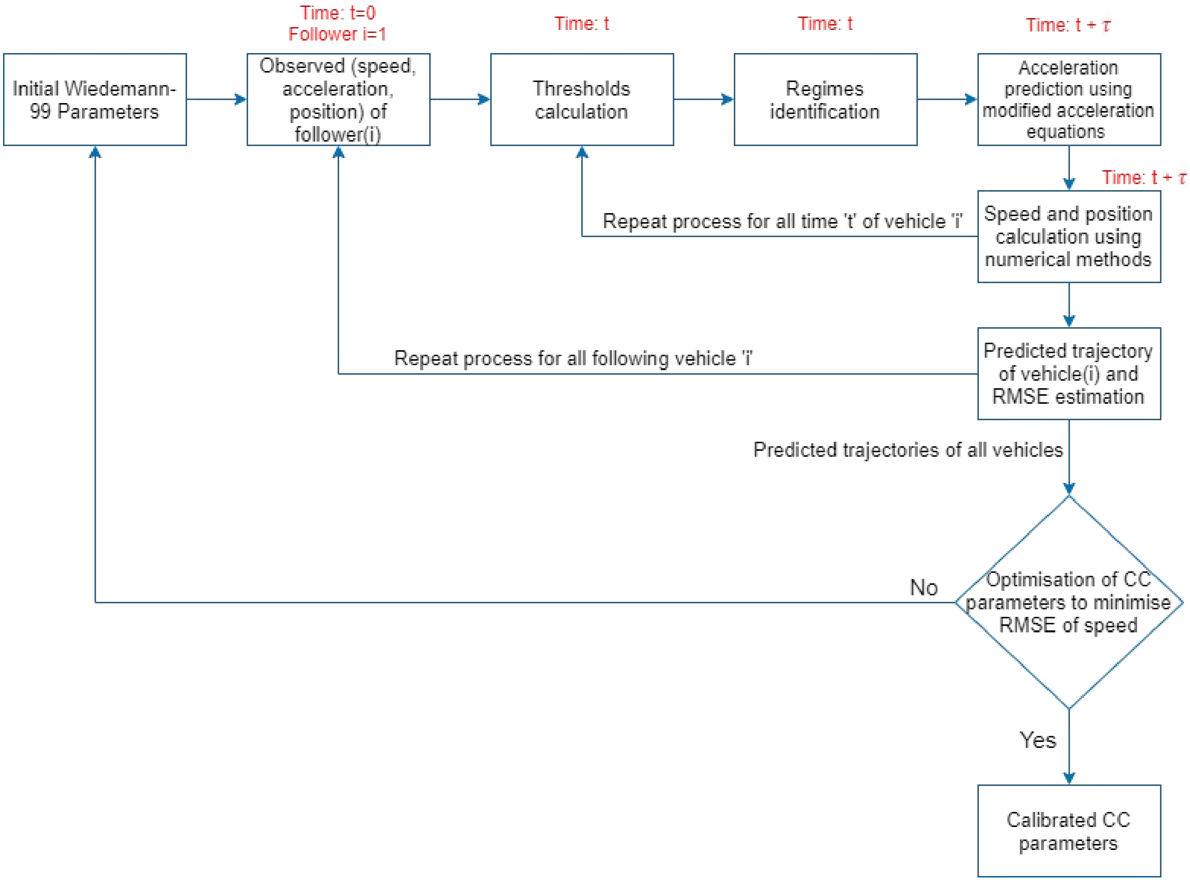

Figure 7. Calibration Methodology

For the assumed initial following parameters (CC), starting time t is set to $t0$ (the initial time when following begins).

Step 1: Perpetual Threshold (as defined in Section 2.1) computations are performed at time t.

Step 2: Based on thresholds in Step 1, regimes are identified at time t.

Step 3: Based on the regimes in Step 2, the acceleration is computed for the follower at time $t + \tau$ (where τ is reaction time) using modified equations given in Section 5.2

Step 4: Speed of the following vehicle is computed at time $t + \tau$ by numerical integration of accelerations in Step 3 using equations given in Section 5.3.

Step 5: The position of the following vehicle is determined at time $t + \tau$ by numerical integration of acceleration in Step 3 and speed in Step 4.

Step 6: The longitudinal gap and speed difference are updated for time $t + \tau$ based on Steps 4 and 5.

Step 7: The time step is incremented.

The above process is repeated to predict all points of the given vehicle and then predicted trajectories of all vehicles for the given set of following parameters.

The deviation between observed and predicted acceleration, speed, and position are computed using root mean squared error (RMSE) for all 'actual' leader-follower pairs. The CC parameters are calibrated by optimizing the Wiedemann model with an objective function to minimize RMSE between observed and predicted speeds.

5.1 Regime Classification Procedure

The clear gap DX and relative speed (follower speed minus leader speed) DV are computed at time *t*, the driving regime of follower at time *t* is determined based on the following conditions as per Aghabayk et al. (*1*)

Case 1: IF [DX(t)>=SDX(t) & DV(t)<=SDV(t)] OR IF [DV(t) <OPDV(t)] then regime at time t is free flow regime

Case 2: IF [DX(t)>ABX(t) & DX(t) < SDX(t) & DV(t) > CLDV(t)] OR IF [DX(t) >=SDX(t) & DV(t) > SDV(t)], then the follower is in closing regime at time t.

Case 3: IF [DX(t)>ABX(t) & DX(t) < SDX(t) & DV(t) > OPDV(t) & DV(t)<=CLDV(t)] then regime at time t is following

Case 4: IF [DV(t) ≥ OPDV(t) & DX (t)≤ ABX(t) & DX(t) > AX(t)], then regime is emergency braking at time t

The threshold equations for the above regime classification are as follows:

$$AX = CC0 \tag{1}$$

$$ABX = CC0 + CC1 * Vslow \tag{2}$$

$$SDX = ABX + CC2 \tag{3}$$

$$CLDV = CC5 + \frac{CC6}{17000} * DX^2 \tag{4}$$

$$OPDV = CC4 - \frac{CC6}{17000} * DX^2 \tag{5}$$

$$SDV = CC5 + \frac{DX - SDX}{CC3} \tag{6}$$

The driving regime at time *t* is identified using the above conditions and thresholds, and for the identified regime, the acceleration is computed for the follower at time *t* + *τ*.

5.2 Modification in Wiedemann Acceleration Equations

The difficulties with existing acceleration equations in the literature and proposed modification are as follows:

i. Free flow regime

The existing acceleration equation in the free-flow regime is

If (DX >ABX)

For v ≤ 22.22 m/s, $B_{max}(t+\tau)=CC8-\frac{(CC8-CC9)*v_n(t)}{22.22}$

(7)

Otherwise, $B_{max}(t+\tau)=CC9$ (8)

If (DX <=ABX)

$B_{max}(t+\tau)=0$ (9)

The existing acceleration equation assumes a constant free-flow speed of 22.22m/s, but it is unrealistic to have the same free-flow speed for all vehicles and road conditions. Also, it assumes that acceleration will be non-negative (CC9) for a speed more than 22.22m/s, but the vehicle should decelerate at higher speeds.

The following equation is used to reflect two modifications:

1. instead of the fixed free-flow speed of 22.22 m/s, vehicle and road type-specific free-flow speed from observed data is considered (using vm_i, which is specific for vehicle type i)
2. the α value is set as 0.4, which ensures that at speeds higher than the road's design speed, acceleration should be negative to achieve the design speed.

$B_{max}(t+\tau)=CC8*\left(1-\frac{(\alpha)*v_n(t)}{vm_i}\right)$

(10)

where $v_n(t)$ = current speed in m/s & vm_i = free-flow speed for vehicle type i in m/s

If (DX <=ABX)

$Bmax(t+\tau)=0$ (11)

ii. Closing regime

The existing acceleration equation is

$B_n(t+\tau)=Max\left(-0.5\frac{DV(t)^2}{DX(t)-ABX(t)},Bmin\right)$

(12)

Where, $B_{min}=-10+\sqrt{(v_n(t))}$ (13)

In the existing equation, when the gap (DX) is close to ABX, then the Bn value increases sharply and will be restricted to B_{min}; this corresponds to an artificial and 'virtually solid wall' at the transition between the following and the emergency braking regime. Also, by the equation of B_{min}, it can have practically unachievable value at lower speeds.

To address these issues, the following modifications are suggested:

1) ABX in the denominator is replaced with CC0, which allows the driver to go closer to the leader than the original formula to match leader speed. This also means that the safety margin is reduced with respect to the original W99 which is partially compensated for by the next

modification. Moreover, we simulated the modification extensively and could not observe accidents.

2) The first term’s denominator is limited to values greater than 0.01m to avoid zero denominators and discontinuous accelerations.
3) B_{min} is treated as a vehicle-specific quantity for mixed traffic.

$$B_n(t+\tau) = Max\left(-0.5\frac{DV(t)^2}{max(DX(t)-CC0,0.01)}, B^i_{min}\right)$$

(14)

B^i_{min} = Max desired deceleration of follower vehicle class i

iii. Following regime

The existing acceleration equation is $B_n(t+\tau) = -CC7$ if the vehicle enters the following regime by crossing CLDV or SDX (i.e., Bn(t)<=0), and $B_n(t+\tau) = CC7$ if it enters the following regime by crossing OPDV or ABX thresholds (i.e., Bn(t)>0).

In the existing acceleration equation, CC7 can take a value greater than B_{max}, which is physically not possible. The modification proposed is:

If DV(t)<0

$$B_n(t+\tau) = min(+CC7, Bmax) \tag{15}$$

If DV(t) >= 0

$$B_n(t+\tau) = -CC7 \tag{16}$$

iv. Emergency braking regime

The existing acceleration equation per (23)is:

$$B_n(t+\tau) = Max\left(-0.5\frac{DV(t)^2}{DX(t)-CC0} + B_{(n-1)}(t), B_{min}\right) \tag{17}$$

Where, $B_{min} = -10 + \sqrt{(v_n(t))}$ (18)

In the existing equation, when the relative speed is near 0, then there are chances of Bn to become positive as the leader can have any acceleration value. Also, it assumes that the driver will decelerate even if the leader is accelerating, i.e., for negative relative speed.

Modifications 2 and 3 from the closing regime are also applicable here. Two more modifications include:

1. For negative relative speed, there is no need for the follower vehicle to decelerate (so acceleration is set to zero).
2. An additional term ($\frac{B_{min} * ABX(t) - DX(t)}{ABX(t) - CC0}$¿, is added to the equation, which gives extra braking motivation when relative speed is near 0 and acceleration computed by the existing equation greater than zero. So, the chance of B_n to become positive when the leader is accelerating is reduced. This term was initially given in W-74 but was removed in W-99.

If DV < 0

B_n (t+τ = 0 (19)

Otherwise,

$$B_n(t+\tau)=Max\left(-0.5\frac{DV(t)^2}{max(DX(t)-CC0,0.01)}+B_{(n-1)}(t),B^i_{min}\right)$$

(20)

If ¿, then

$$Bn(t+\tau)=Max\left(-0.5\frac{DV(t)^2}{max(DX(t)-CC0,0.01)}+B_{(n-1)}(t)+\frac{B_{min}*ABX(t)-DX(t)}{ABX(t)-CC0},B^i_{min}\right)$$

(21)

B^i_{min}= Max desired deceleration of following vehicle class.

Once the acceleration values are estimated for the regimes, the speed and position are calculated using numerical integration methods.

5.3 Numerical Integration Methods for Speed and Position Calculation:

For calculation of speed and position from acceleration, numerical integration equations are used. Several popular methods such as the Euler Cromer method, Midpoint method, Velocity Verlet method, and Beeman method have been reported in the literature to be suitable for computing speed and positions from Newton's equation of motion (*33*). The most appropriate can be problem-specific and needs to be evaluated on the desired dataset. Thus, these numerical integration methods are applied to predict leaders' speeds and positions based on observed acceleration profiles. The results are discussed in Section 6.3.

The equations for various methods are shown below:(*33*)

Euler Cromer Method:

$$v(t+1)=v(t)+B(t)*dt \quad (22)$$

$$x(t+1)=x(t)+v(t+1)*dt \quad (23)$$

Midpoint Method:

$$v(t+1)=v(t)+B(t)*dt \quad (24)$$

$$x(t+1)=x(t)+\frac{1}{2}[v(t)+v(t+1)]*dt \quad (25)$$

Velocity Verlet Method:

$$v(t+1)=v(t)+\frac{1}{2}[B(t)+B(t+1)]*dt \quad (26)$$

$$x(t+1)=x(t)+v(t)*dt+\frac{1}{2}B(t)*dt^2 \quad (27)$$

Beeman Method:

$$v(t+1)=v(t)+\frac{1}{6}[2B(t+1)+5B(t)-B(t-1)]*d\mathrm{t} \quad (28)$$

$$x(t+1)=x(t)+v(t)*dt+\frac{1}{6}[4B(t)-B(t-1)]*dt^2 \quad (29)$$

where,

v(t+1) – speed at next time step

x(t+1) – position at next time step

B(t) – acceleration at current time step

B(t+1) – acceleration at next time step

B(t-1) – acceleration at previous time step

dt – time step.

5.4 The Goodness of Fit Function Used for Calibration

The goodness of fit function for calibration is the deviation between observed and computed speeds. Thus, calibration is formulated as an optimization problem to determine the best set of model parameter values, which minimizes this RMS error.

$$\text{Min } Z = \text{RMSE (inst.speed)} = \frac{\sum_{i=1}^{N}\sqrt{\frac{1}{T}\sum_{t=1}^{T}\left(speed_{deviation}(i,t)\right)^2}}{N}; \quad (30)$$

$$speed_{deviation}(i,t)=v^{obs}(i,t)-v^{pred}(i,t)$$

$v^{pred}(i,t)$ is obtained from numerical integration of B(i,t) as per equation 28. B(i,t) is a non-linear function $f(CC, DV, DX, V, B)$, as given in section 5.2

Thus $v^{pred}(i,t)$ is $f(CC0, CC1, CC2, \ldots\ldots.., CC9)$ but is non-smooth and non-differentiable due to the presence of maxima and minima. Hence analytical optimization techniques cannot be used. The optimization is done using the metaheuristics such as the Nelder-Mead method in R-studio software.

In this study, out of 10 W-99 parameters (CC0-CC9), Seven parameters are calibrated. CC1, CC2, CC3, CC4, CC5, CC7, and CC8 are calibrated. CC0 is determined by measuring the gaps in a drone image of the stopped vehicles at a signal. CC0 for TW is taken as 0.4m, and 0.66m for cars, the default value of CC6 is adopted in this study like in Raju et al. (6) Durrani et al. *(7),* and CC9 is not used in the modified equations.

Other fixed values used in calibration include the desired speed, maximum deceleration rates (cf. Table 2), and the reaction time (τ) is taken as 1.0 s. based on empirical analysis conducted by authors.

The optimization-based calibration process determines a set of CC parameters for a given class that yields the minimum RMSE. This procedure is done separately for the vehicle classes TW and cars. For the calibrated values of cc parameters, RMS errors for acceleration and position are also computed based on the deviation between the observed and predicted values.

6. Results and Discussion

6.1 Analysis Methodology

For the calibration and validation purpose, leader-follower pairs are randomly divided into 70% (Pairs: TW=250, Car=200 with Datapoints: TW=6710, Car=5748) for the estimation and 30% holdout data for the validation. The model is calibrated using the estimation dataset and validate by calculating performance measures with the calibrated model on the holdout dataset.

This study is analyzed as per the following methodology:

i) The W-99 model is calibrated by using existing acceleration equations and proposed acceleration equations to evaluate the effect of equations' modifications.

ii) Alternative numerical integration schemes are evaluated to find the method which gives accurate predictions for acceleration, speed, and position over time.

iii) The proposed W-99 calibrated model is compared with other calibrated W-99 models by evaluating the performance measures, RMSE of acceleration, instantaneous speed, and position.

iv) Different driving behavior of TW and cars are evaluated from their CC-values and Gap-Relative speed plot.

v) Leader-follower pairs are classified into Strict and overlapping staggered following based on the lateral overlap, and calibration analysis is done for these pairs.

Table 3 shows the calibrated CC parameter by existing acceleration equation and proposed acceleration equations, CC parameters by heuristic methods, and goodness of fit of these parameters and for validation data set for TW and cars.

Table 3 Calibrated CC parameters and Goodness of Fit using existing and proposed acceleration equations and heuristic methods.

Two-Wheeler						Car				
Parameters	Existing Acceleration (optimization)	Proposed acceleration (Optimization)	Validation	Heuristic 1 (w/o Optimization) (6)	Heuristic 2 (w/o Optimization) (7)	Existing n Acceleration (optimization)	Proposed Acceleration (Optimization)	Validation	Heuristic 1 (w/o Optimization) (6)	Heuristic 2 (w/o Optimization) (7)
CC1 (s)	1.78	1.39	Same as column 2	0.81	1.021	1.13	1.48	Same as column 7	0.76	0.96
CC2 (m)	8.27	9.75		7.66	5.29	11.62	14.02		7.74	5.687
CC3 (s)	-11	-9.45		-8	-5.9	-6.94	-11.4		-12.11	-6.18
CC4 (m/s)	-0.84	-1.56		-1.65	2.69	-0.9	-1.95		-1.78	-2.7
CC5 (m/s)	1.14	1.31		2.04	2.692	1.11	1.61		1.99	2.7
CC7 (m/s^2)	0.3	0.29		0.24	0.24	0.26	0.33		0.24	0.24
CC8 (m/s2)	3	2.78		3	3	3.15	3.15		3.15	3.15
RMSE (Acceleration) m/s2	1.17	1.08	1.01	1.4	1.67	1.21	1.08	0.97	1.26	1.47
RMSE (Inst Speed) m/s	1.9	1.56	1.49	2.51	3.26	2.99	1.64	1.45	2.16	3.74
RMSE (Position) m	7.96	5.25	4.96	9.09	11.63	12.3	7.79	5.6	9.58	16.85

The results of calibration by existing acceleration equations (columns 1 and 6) and by proposed acceleration equations (columns 2 and 7) are explained in Section 6.2

The results of calibration by Heuristic 1 (column 4 and column 9) and Heuristic 2(column 5 and column 10) are explained in Section 6.4

Performance on the holdout set

For the holdout data (30%), the performance measures are computed using the CC parameters obtained after calibration using the proposed equations; the result is given in columns 3&8 in Table 3. From the results, the calibrated model parameters also perform well on the validation dataset.

6.2 Use of Modified Acceleration Equations

Position, speed, and acceleration profiles predicted by existing acceleration equations and the proposed acceleration equation are plotted along with observed profiles for a sample follower in the following Figure 8.

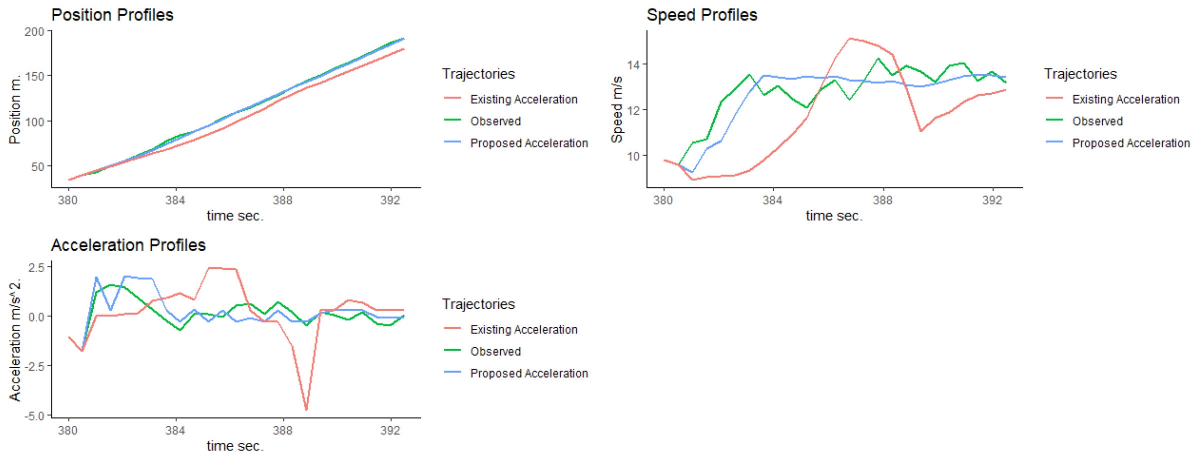

Figure 8. Trajectory Profiles with modified and existing acceleration equations

From Figure 8, the model with proposed acceleration equations predicts the observed trajectories better than the model with existing acceleration equations. This is also observed in Table 3, where RMSE of the proposed acceleration equations are lower for speed (RMSE (m/s): 1.56 vs. 1.9), position (RMSE (m): 5.25 vs. 7.96), and acceleration (RMSE (m/s^2): 1.08 vs. 1.17) than for the existing equations for two-wheelers. Similar trends are observed for cars as well.

6.3 Evaluation of Numerical Integration Methods for Trajectory Computation

Numerical integration methods from section 5.3 are evaluated based on deviation speed and position profiles relative to the observed trajectories. Figure 9 (a) and (b) shows the plot of absolute deviation of speed and absolute deviation of position by the different methods with observed speed and position of a sample leader respectively. The goodness of fit is measured by the root mean square error (RMSE) of predictions.

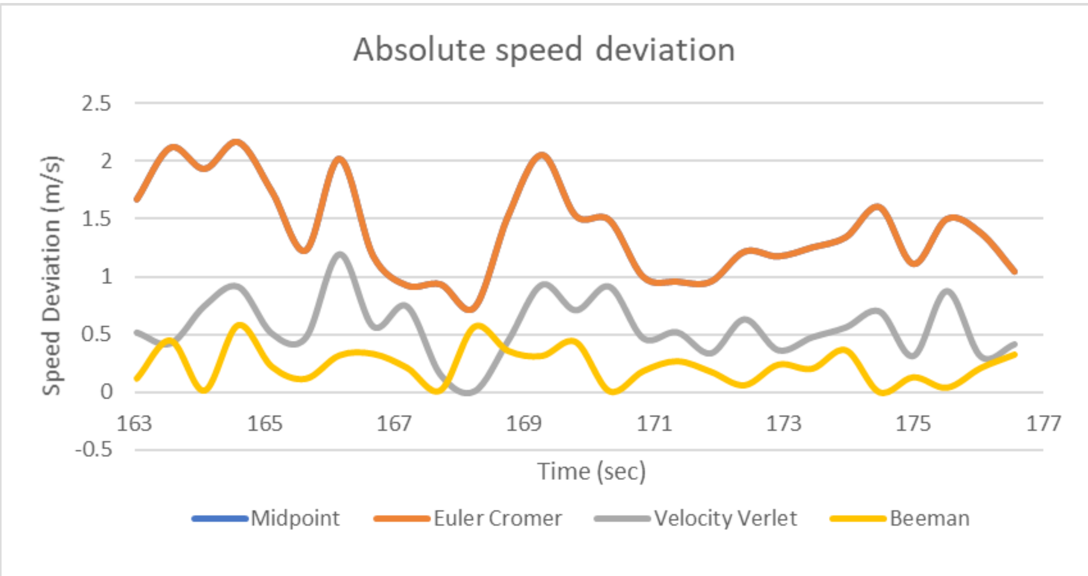

Figure 9 (a). Absolute speed deviation for different numerical integration methods

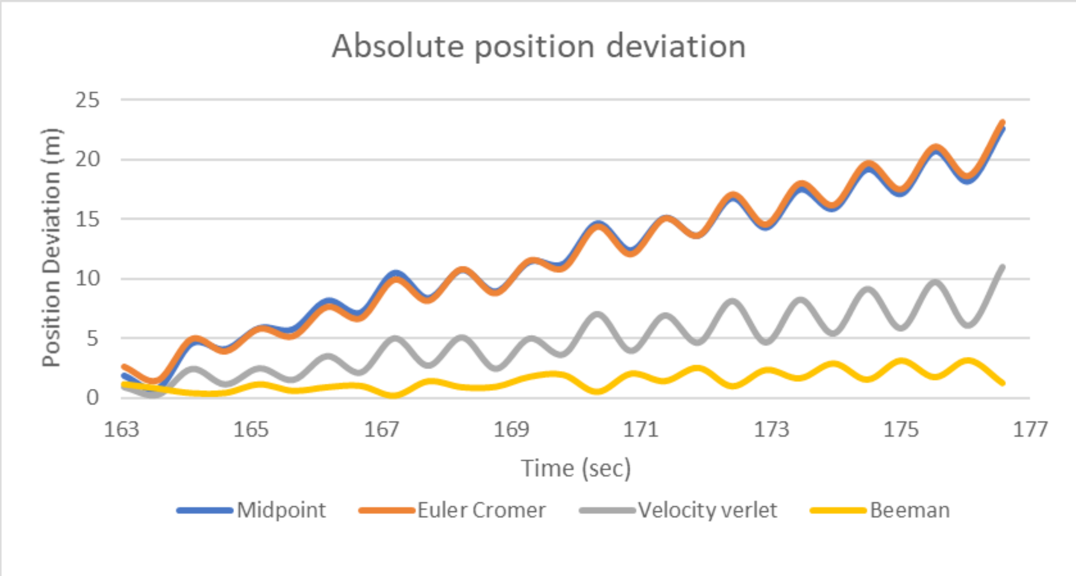

Figure 9 (b). Absolute position deviation for different numerical integration methods

The average RMSE between observed values and calculated values of speed & position are computed for all different methods across all different leaders.

RMSE of speed for Midpoint Method: 1.438 m/s, Euler Cromer Method: 1.438 m/s, Velocity Verlet Method: 0.606 m/s, and for Beeman Method: 0.282 m/s.

RMSE of position for Midpoint Method: 12.701 m, Euler Cromer Method: 12.701 m, Velocity Verlet Method: 5.345 m, and for Beeman Method: 1.692 m.

The RMSE is smallest for Beeman's method for both speed and position computations and hence this method is used subsequently.

6.4 Comparison with other W-99 Models

W-99 parameters are calibrated for the given dataset using procedures provided by Raju et al. (*6*) and Durrani et al. (*7*), denoted as the heuristic method 1 and 2, respectively. The heuristic 1 method is chosen because they have used the same data as in this paper to calibrate the W-99 model; heuristic 2 is considered as they have considered heterogeneity across the vehicle types and pairs. As noted earlier, these heuristic methods calculate W-99 parameters without minimizing the deviation from observed field data.

For comparison, the proposed parameters and fit functions were compared with other calibration results in the literature for multi-lane mixed traffic conditions based on macroscopic performance measures.

Following Fig.10 shows the deviation of the sample predicted trajectory of the follower (TW) by different W-99 models with observed trajectory.

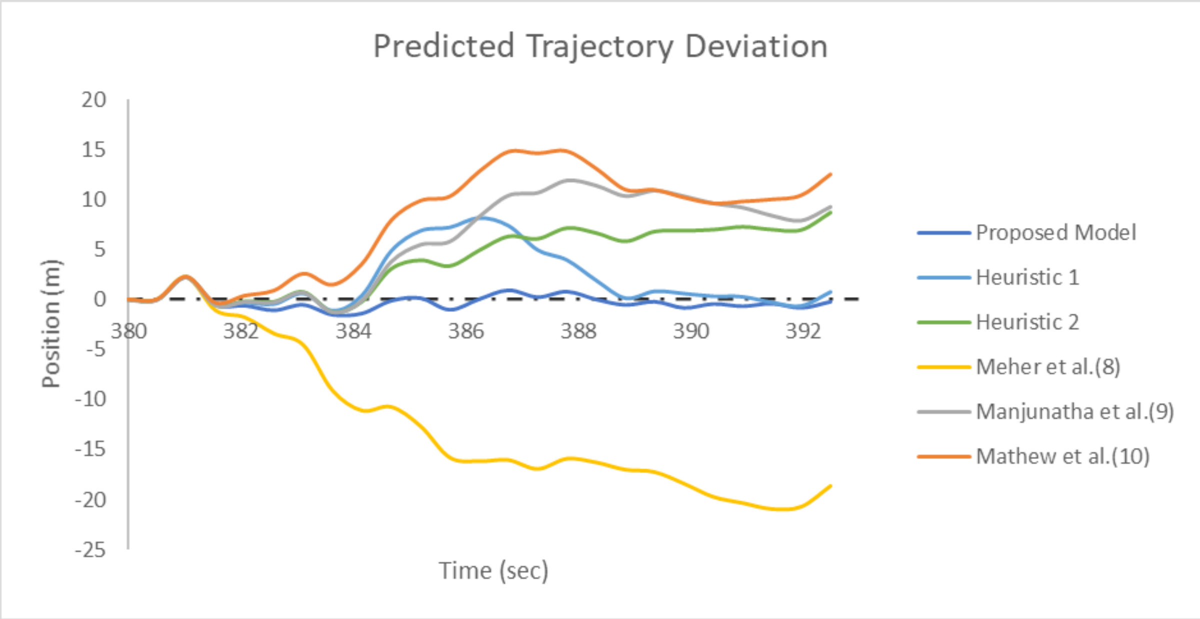

Figure 10. Predicted Trajectory Deviation

The results of performance measures by the proposed model, heuristic models, and other calibration results in the literature are plotted in Figure 11.

Following plot 11 (a), (b), (c) shows the RMSE of acceleration, speed, and position respectively for different calibrated W-99 Models for TW as a class of follower.

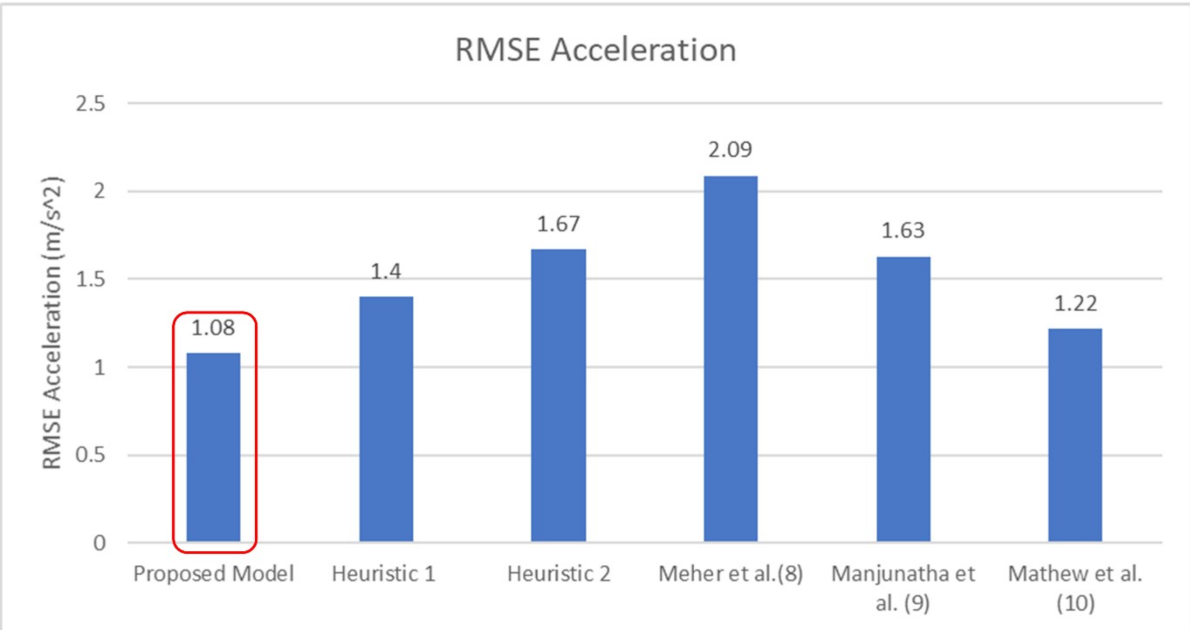

Figure 11 (a) RMSE Acceleration for different W-99 Models

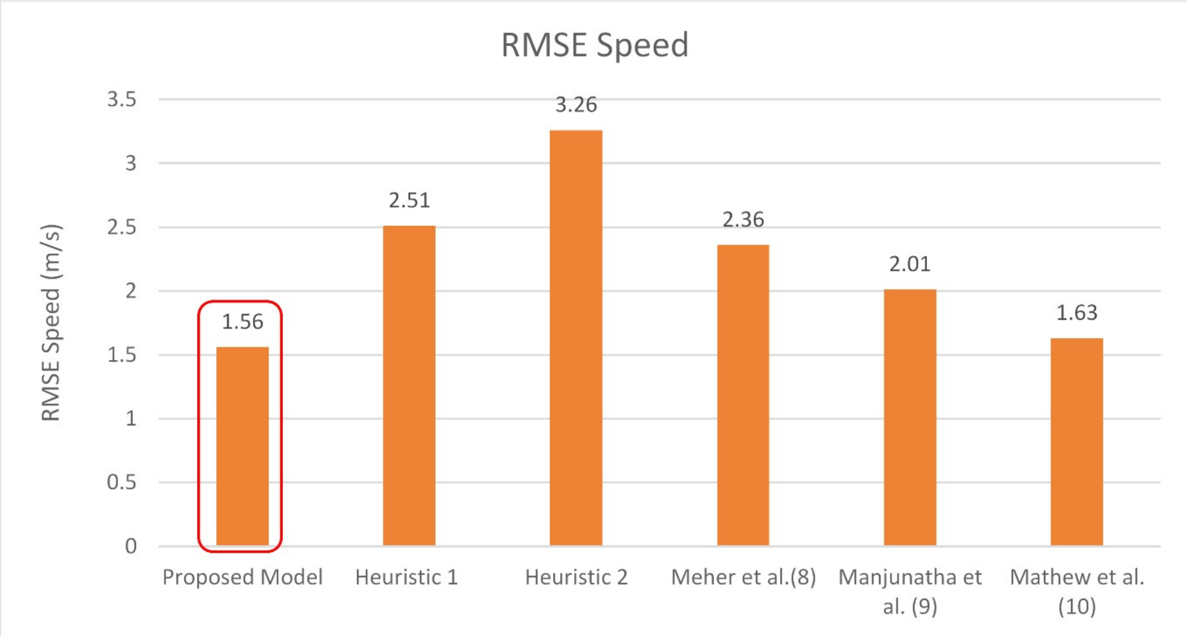

Figure 11 (b) RMSE Speed for different W-99 Models

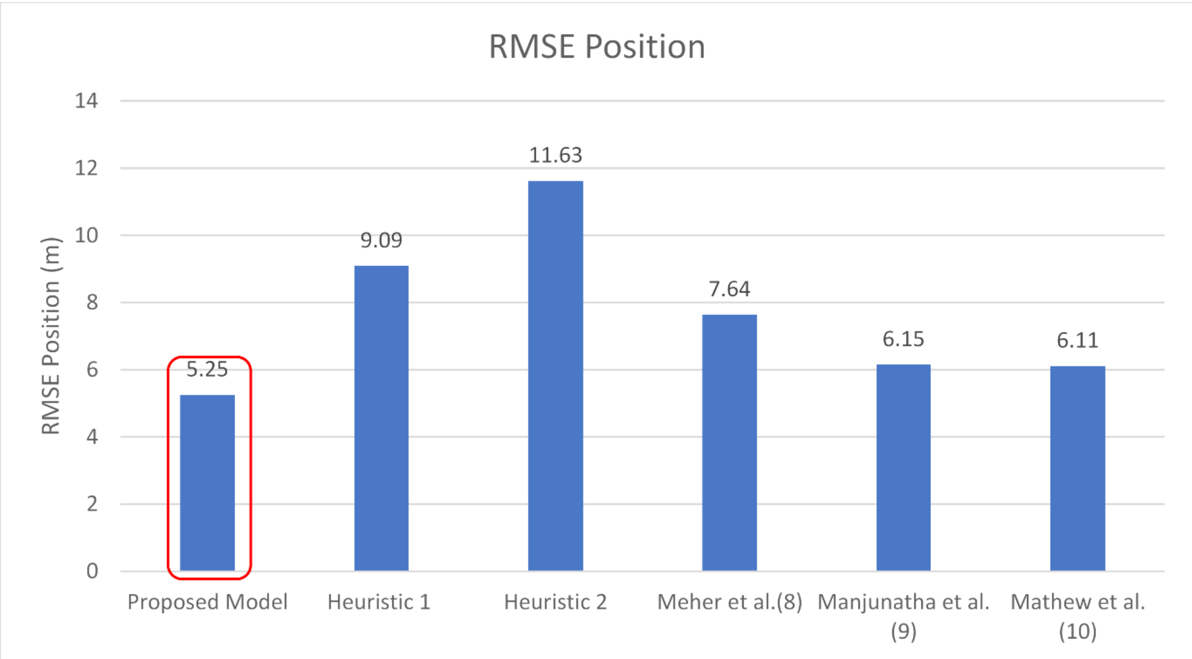

Figure 11 (c) RMSE Position for different W-99 Models

From the above RMSE results, it can be seen that the performance measures by the proposed method offer a significant improvement in predicting acceleration, speed, and positions at the microscopic level.

6.5 Difference in Vehicle-Following Parameters and Thresholds between TW and Car

Figure 12 shows the gap-relative speed plots with thresholds of regime identification, calculated for the CC parameters by the proposed method is given in Table 3, for a constant leader speed of 10 m/s.

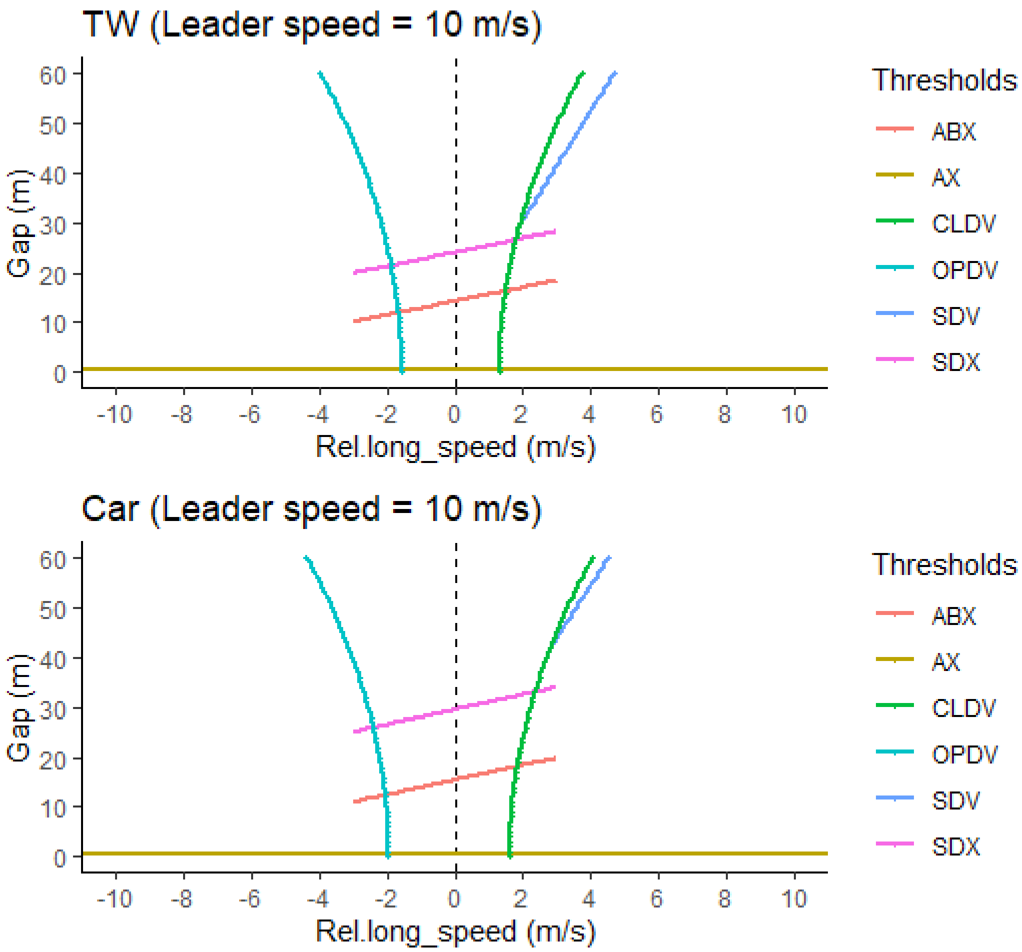

Figure 12 Wiedemann Threshold Plots for TW and Car

From the calibrated W-99 parameters for TW and cars in Table 3 (columns 2 and 7) and threshold plots of the same parameters in Figure12, we can see that the threshold diagram and the CC parameters are quantitatively different for these two vehicle classes.

CC1 of cars is larger than that for TW, which is evident as car drivers keep more gap to the leader than TW. Hence, ABX for TW will be lower than that for cars. Consequently, a lower percentage of TW points will be in the emergency braking regime than is the case for cars.

CC2 decides the range of the following regime; the value difference shows that cars have a longer following regime than TW, as SDX will be higher. Hence, car drivers can sense the change in leader behavior at a longer gap than TW drivers. Consequently, the chance of TW drivers being in the free-flow regime is higher compared to that of car drivers.

CC3 for TW is lower in magnitude than that for cars, which we can see as the slope of the SDV line in the threshold plot; hence TW drivers perceive a slow-moving leader and decelerate earlier than car drivers.

CC4 & CC5 gives the OPDV & CLDV thresholds; for TWs, both CC4 and CC5 are smaller in magnitude than that for cars; hence TW is more sensitive to change in leader's speed.

CC7 is acceleration in the following regime; car drivers apply higher acceleration values than TW drivers while following the leader unconsciously.

The most important observation is that, under the same relative speed and gap stimulus, two-wheelers, and cars may be in different regimes and display different acceleration responses. Thus, accurate calibration of each vehicle's parameters is essential for developing micro-simulation models for mixed traffic.

6.6 Analysis of Following Behavior between Strict and Overlapping-Staggered Following

A follower is considered to belong to the strict following regime if its overlapping width is more than 0.25m for TW and more than 0.75m for cars (i.e., 50% of the average width) for at least half of the observed time interval or if the smaller of the pair has a full overlap. Otherwise, the follower is considered to be in the overlapping-staggered following regime, these criteria are based on empirical analysis conducted by authors. 276 two-wheelers and 328 cars were in the strict following regime, whereas 268 two-wheelers and 152 cars were classified into the staggered following regime. The calibration analysis is done for strict and overlapping-staggered. The calibrated parameters and the Goodness of fit [RMSE (acceleration) m/s^2, RMSE (speed) m/s, RMSE (position) m] for the above four sets of CC's are given in Table 4.

Table 4 Calibrated CC parameters and Goodness of Fit for Strict and Overlapping Staggered following

Parameter	TW		Car	
	Strict Following	Overlapping Staggered Following	Strict Following	Overlapping Staggered Following
Pairs	276	268	328	152
CC1	1.32	1.13	1.48	1.13
CC2	10.1	11.97	11.02	13
CC3	-9.09	-10.02	-10.4	-10.67
CC4	-1.84	-1.64	-1.8	-1.7
CC5	1.38	1.31	1.56	1.47
CC7	0.29	0.29	0.26	0.35
CC8	2.33	2.57	2.91	3.11
RMSE Acceleration (m/s^2)	0.97	1.1	0.94	1.11
RMSE Speed (m/s)	1.46	1.6	1.41	1.65
RMSE Position (m)	4.88	5.26	5.17	7.52

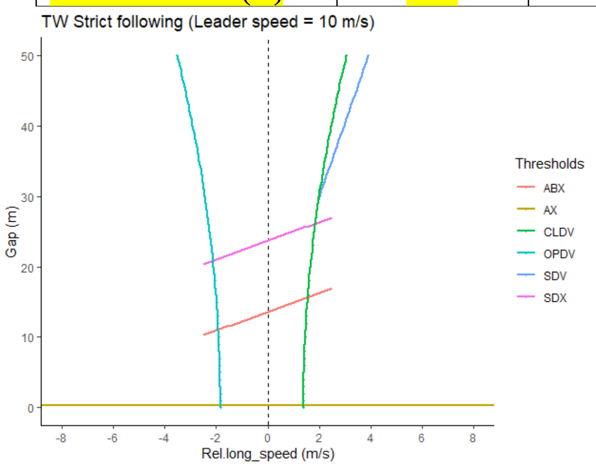

Figure 13 (a) Wiedemann Threshold Plots - Strict following for TW and cars

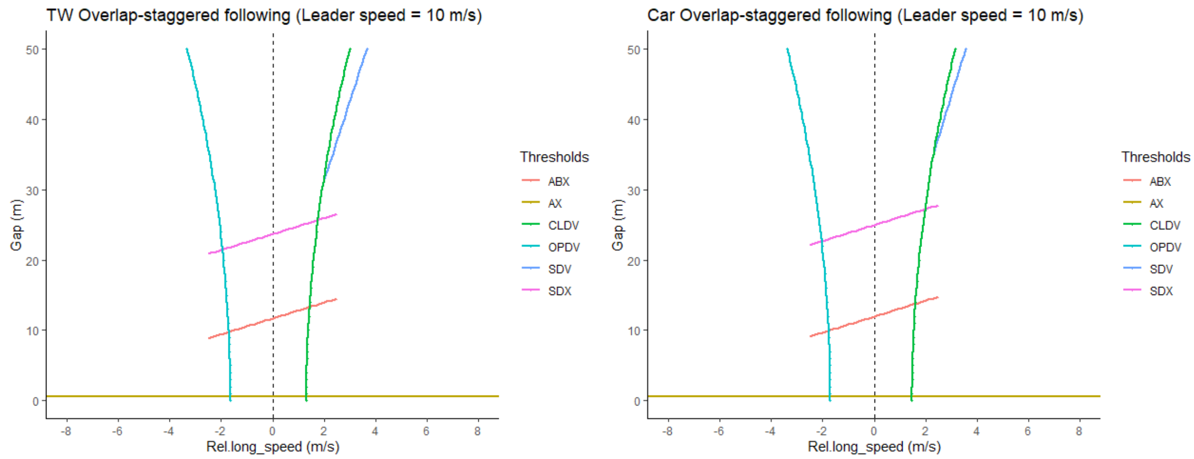

Figure 13 (b) Wiedemann Threshold Plots - Overlapping-Staggered following for TW and cars

Figure 13 (a) and (b) shows the gap-relative speed plots with thresholds of regime identification for the CC parameters of Strict and Overlap-Staggered following for TW and car as given in Table 4 respectively, for a constant leader speed of 10 m/s.

The calibration results indicate that the driving behavior in a staggered car-following situation is different from that of strict car-following. This is particularly true for the safety indicator time to collision, i.e., the ratio of gap (DX) and relative speed (DV) (*34*) Therefore, different parameter sets are to be calibrated for strict and staggered following.

The CC1 values for strict and staggered following imply that drivers keep a smaller gap in staggered following compared to the strict following. The found CC4 and CC5 values imply that, in the staggered following, drivers are more sensitive to changes in leader's speed than the strict following. There are also differences with respect to the vehicle classes: TW drivers are found to keep lower gaps and to be more sensitive to speed changes of a leader than car drivers.

7. CONCLUSION

This paper proposes and implements a calibration procedure for the Wiedemann-99 model based on RMSE between simulated and observed trajectories of mixed traffic consisting predominantly of motorized two-wheelers and cars. The proposed modifications of the Wiedemann acceleration equations allowed for a more realistic representation of driving behavior under these conditions. Alternative numerical integration schemes for computing speed and position over time are evaluated. The performance of the proposed calibration method is compared with other heuristic trajectory-based calibration methods. The calibrated parameters may help understand the dynamics of mixed traffic flow. Particularly, we found differences in the car-following behavior between motorized two-wheelers and cars as well as between strict and overlapping staggered following.

The following key findings and observations emerge from this study. The simulation-based analysis demonstrates that different microscopic W-99 parameters can lead to similar macroscopic performance measures. Thus, the psychophysical (Wiedemann model) calibration using macroscopic and aggregate performance measures may not uniquely determine microscopic behavior or performance.

Existing acceleration equations reported in the context of W-99 models can lead to some inconsistency and unrealistic driving behavior characteristics. These include the inability to capture vehicle type-specific features and a wrong sign for acceleration in some cases. Modifications are proposed to these equations to be consistent with observed driving behavior.

The microscopic performance of the above model in computing trajectories depends on the calibration parameters and is also quite sensitive to the numerical integration technique. Five different methods were evaluated, and it was observed that Beeman's integration scheme provides the best fit with the observed data.

An optimization-based scheme is used to calibrate the W-99 model for mixed traffic with the above modifications. The proposed calibration scheme is found to outperform other calibration methods based on trajectory data (but without optimization) in terms of RMS errors for speed, position, and acceleration. The calibrated parameter values for thresholds and boundaries for regimes turned out to be behaviourally more realistic than those produced with other methods. Visual comparison of the regimes across models confirms these differences.

Not only do the parameters and the regime boundaries vary across calibration methods, but they also differ between two-wheelers and cars in mixed traffic. These differences are quantified and illustrated using sample plots of relative speed and gap across vehicle classes. The results reveal that the calibrated parameter values and, consequently, the thresholds that delineate closing, following, emergency braking, and opening regimes vary between two-wheelers and cars. The window (in the relative speed vs. gap plot) for the unconscious following is larger for cars, while the free flow regime is more extensive for two-wheelers. Under the same relative speed and gap stimulus, two-wheelers and cars may be in different regimes and display different acceleration responses.

The study's findings have direct and vital applications for the calibration and development of mixed traffic micro-simulation models. This study is based on calibration from a mid-block section in a divided six-lane arterial in Chennai. Extending this study to other locations and considering extended car-following behavior such as vehicle platooning case is a direction for continuing research. Extending the analysis to consider other facility types (four-lane divided urban roads, two-lane divided and undivided roads) as well as intersections by choosing suitable performance measures is an exciting and challenging direction for future work.

This work can be extended to other simulation platforms, including Sumo, Aimsun, Simtraffic, etc. since all models belong to the same class of car-following models (local time-continuous models or iterated maps with speed, relative speed, gap, and sometimes acceleration as exogenous variables). More systematic studies that relax the conditions to identify leader-follower pairs (in terms of duration of the following or extent of lateral overlap) allowing to analyse more diverse leader-follower pairs are being investigated currently by the authors and will be reported in future studies. Furthermore, the analysis can be extended to model, not just the leader but the whole local traffic environment as explicit input allowing for many other maneuvers beyond this particular study's scope.

ACKNOWLEDGMENT

This work is supported by scholarships through MHRD Government of India and DAAD (The German Academic Exchange Service) fellowship at TU Dresden, which is gratefully acknowledged. The authors express sincere thanks to four anonymous reviewers for their constructive suggestions.

AUTHOR CONTRIBUTIONS

The authors confirm contribution to the paper as follows:
Study Conception and Design: A. Chaudhari, K. Srinivasan, B. Chilukuri, M. Treiber, O. Okhrin
Analysis and interpretation: A. Chaudhari, K. Srinivasan, B. Chilukuri, M. Treiber, O. Okhrin.

Draft manuscript preparation: A. Chaudhari, K. Srinivasan, B. Chilukuri, M. Treiber, O. Okhrin
All authors reviewed the results and approved the final version of the manuscript.

References

1. Aghabayk, K., M. Sarvi, W. Young, and L. Kautzsch. A Novel Methodology For Evolutionary Calibration Of Vissim By Multi-Threading. Australasian Transport Research Forum Proceedings, 2013.
2. Olstam, J. J., and A. Tapani. Comparison of Car-Following Models. 2004.
3. Vortisch, P. Wiedemann-99 Source Code. https://www.researchgate.net/post/Where-I-can-find-the-mathematical-formulation-of-Wiedemann-99-car-following-model. Accessed Feb. 2, 2021.
4. Menneni, S. Pattern Recognition Based Microsimulation Calibration and Innovative Traffic Representations. Ph.D. Thesis. 2008
5. Rrecaj, A. A., and K. M. Bombol. Calibration and Validation of the VISSIM Parameters-State of the Art. TEM Journal, Vol. 4, No. 3, 2015, pp. 255–269.
6. Raju, N., S. Arkatkar, and G. Joshi. Modeling Following Behavior of Vehicles Using Trajectory Data under Mixed Traffic Conditions: An Indian Viewpoint. Transportation Letters, 2020. https://doi.org/10.1080/19427867.2020.1751440.
7. Durrani, U., C. Lee, and H. Maoh. Calibrating the Wiedemann's Vehicle-Following Model Using Mixed Vehicle-Pair Interactions. Transportation Research Part C: Emerging Technologies, Vol. 67, 2016, pp. 227–242. https://doi.org/10.1016/j.trc.2016.02.012.
8. Mehar, A., S. Chandra, and S. Velmurugan. Highway Capacity through Vissim Calibrated for Mixed Traffic Conditions. KSCE Journal of Civil Engineering, Vol. 18, No. 2, 2014, pp. 639–645. https://doi.org/10.1007/s12205-014-0440-3.
9. Manjunatha, P., P. Vortisch, and Mathew T. v. Methodology for the Calibration of VISSIM in Mixed Traffic. Transportation Research Record, 2013.
10. Mathew, T. v, and P. Radhakrishnan. Calibration of Microsimulation Models for Nonlane-Based Heterogeneous Traffic at Signalized Intersections. Transportation Letters: The International Journal of Transportation Research, Vol. 3, 2011, pp. 113–126. https://doi.org/10.1061/ASCE0733-94882010136:159.
11. Bhattacharyya, K., B. Maitra, and M. Boltze. Calibration of Micro-Simulation Model Parameters for Heterogeneous Traffic Using Mode-Specific Performance Measure. Transportation Research Record, Vol. 2674, No. 1, 2020, pp. 135–147. https://doi.org/10.1177/0361198119900130.
12. Maheshwary, P., K. Bhattacharyya, B. Maitra, and M. Boltze. ScienceDirect A Methodology for Calibration of Vehicle Class-Wise Driving Behavior in Heterogeneous Traffic Environment. World Conference on Transport Research - WCTR Shanghai. 2016
13. Kanagaraj, V., G. Asaithambi, C. H. N. Kumar, K. K. Srinivasan, and R. Sivanandan. Evaluation of Different Vehicle Following Models Under Mixed Traffic Conditions. Procedia - Social and Behavioral Sciences, Vol. 104, 2013, pp. 390–401. https://doi.org/10.1016/j.sbspro.2013.11.132.

14. Kashyap N. R, M., B. R. Chilukuri, K. K. Srinivasan, and G. Asaithambi. Analysis of Vehicle-Following Behavior in Mixed Traffic Conditions Using Vehicle Trajectory Data. Transportation Research Record, Vol. 2674, No. 11, 2020, pp. 842–855. https://doi.org/10.1177/0361198120949874.

15. Kanagaraj, V., and M. Treiber. Self-Driven Particle Model for Mixed Traffic and Other Disordered Flows. Physica A: Statistical Mechanics and its Applications, Vol. 509, 2018, pp. 1–11. https://doi.org/10.1016/j.physa.2018.05.086.

16. Anand, P. A., P. Atmakuri, V. S. R. Anne, G. Asaithambi, K. K. Srinivasan, R. Sivanandan, and B. R. Chilukuri. Calibration of Vehicle-Following Model Parameters Using Mixed Traffic Trajectory Data. Transportation in Developing Economies, Vol. 5, No. 2, 2019. https://doi.org/10.1007/s40890-019-0086-4.

17. Asaithambi, G., V. Kanagaraj, K. K. Srinivasan, and R. Sivanandan. Study of Traffic Flow Characteristics Using Different Vehicle-Following Models under Mixed Traffic Conditions. Transportation Letters, Vol. 10, No. 2, 2018, pp. 92–103. https://doi.org/10.1080/19427867.2016.1190887.

18. Anand, A., G. Ramadurai, and L. Vanajakshi. Data Fusion-Based Traffic Density Estimation and Prediction. Journal of Intelligent Transportation Systems: Technology, Planning, and Operations, Vol. 18, No. 4, 2014, pp. 367–378. https://doi.org/10.1080/15472450.2013.806844.

19. Siddharth, S. M. P., and G. Ramadurai. Calibration of VISSIM for Indian Heterogeneous Traffic Conditions. Procedia - Social and Behavioral Sciences, Vol. 104, 2013, pp. 380–389. https://doi.org/10.1016/j.sbspro.2013.11.131.

20. Mathew, T. v., and K. V. R. Ravishankar. Car-Following Behavior in Traffic Having Mixed Vehicle-Types. Transportation Letters, Vol. 3, No. 2, 2011, pp. 109–122. https://doi.org/10.3328/TL.2011.03.02.109-122.

21. Punzo, V., B. Ciuffo, and M. Montanino. Can Results of Car-Following Model Calibration Based on Trajectory Data Be Trusted? Transportation Research Record, No. 2315, 2012, pp. 11–24. https://doi.org/10.3141/2315-02.

22. Wiedemann, R. Simulation Des Straßenverkehrsflusses. Instituts für Verkehrswesen der Universität Karlsruhe, Heft 8, Karlsruhe, Germany, 1974.

23. Higgs, B., M. Abbas, and A. Medina. Analysis of the Wiedemann Car Following Model over Different Speeds Using Naturalistic Data. 3rd International Conference on Road Safety and Simulation, 2011.

24. Sharma, A., Z. Zheng, and A. Bhaskar. Is More Always Better? The Impact of Vehicular Trajectory Completeness on Car-Following Model Calibration and Validation. Transportation Research Part B 120C, 2019, pp. 49–75.

25. Pourabdollah, M., E. Bjarkvik, F. Furer, B. Lindenberg, and K. Burgdorf. Calibration and Evaluation of Car Following Models Using Real-World Driving Data. IEEE Conference on Intelligent Transportation Systems, Proceedings, 2018, pp. 1–6

26. Ranjitkar P, Nakatsuji T, and Asano M. Performance Evaluation of Microscopic Flow Models with Test Track Data. Transportation Research Record, 2004, pp. 90–100.

27. Gipps, P. G. A BEHAVIOURAL CAR-FOLLOWING MODEL FOR COMPUTER SIMULATION. Transportation Research board, Vol. 15B,2, 1981, pp. 403–414.

28. Treiber, M., A. Hennecke, and D. Helbing. Congested Traffic States in Empirical Observations and Microscopic Simulations. Physical Review E - Statistical Physics, Plasmas, Fluids, and Related Interdisciplinary Topics, Vol. 62, No. 2, 2000, pp. 1805–1824. https://doi.org/10.1103/PhysRevE.62.1805.

29. Krauss, S. Microscopic Modeling of Traffic Flow: Investigation of Collision Free Vehicle Dynamics. PhD Thesis, University of Cologne, 1997.

30. Chaudhari, A. A. Methodology and Calibration of Psychophysical Type Wiedemann Parameters for Mixed Traffic Flow Using Vehicular Trajectory Data. Chennai, 2020.

31. Kanagaraj, V., G. Asaithambi, T. Toledo, and T. C. Lee. Trajectory Data and Flow Characteristics of Mixed Traffic. Transportation Research Record, Vol. 2491, 2015, pp. 1–11. https://doi.org/10.3141/2491-01.

32. Arasan, V. T., and R. Z. Koshy. Methodology for Modeling Highly Heterogeneous Traffic Flow. Journal of Transportation Engineering, ASCE., Vol. 131, 2005, pp. 544–551. https://doi.org/10.1061/ASCE0733-947X2005131:7544.

33. Gould, H., J. Tobochnik, and W. Christian. An Introduction to Computer Simulation Methods Applications to Physical System. 2016.

34. Treiber, M., and A. Kesting. Traffic Flow Dynamics: Data, Models and Simulation. Springer Berlin Heidelberg, 2013.

Figure Legends:

1. Figure 1 Schematic representation of Wiedemann Model (*22*)
2. Figure 2. Wiedemann thresholds plots for different sets of CC parameters
3. Figure 3. Trajectory Plots of Simulated Data for different sets of CC parameters
4. Figure 4. Snapshot of study section (*31*)
5. Figure 5. Trajectories Plot
6. Figure 6 (a). Gap-Relative speed plot displaying hysteresis Behaviour
7. Figure 6 (b). Gap-Relative speed plot displaying non-hysteresis Behaviour
8. Figure 7. Calibration Methodology
9. Figure 8. Trajectory Profiles with modified and existing acceleration equations
10. Figure 9 (a). Absolute speed deviation for different numerical integration methods
11. Figure 9 (b). Absolute position deviation for different numerical integration methods
12. Figure 10. Predicted Trajectory Deviation
13. Figure 11 (a). RMSE Acceleration for different W-99 Models
14. Figure 11 (b). RMSE Speed for different W-99 Models
15. Figure 11 (c). RMSE Position for different W-99 Models
16. Figure 12 Wiedemann Threshold Plots for TW and Car

17. Figure 13(a). Wiedemann Threshold Plots Strict following for TW and cars
18. Figure 13(b). Wiedemann Threshold Plots Overlapping-Staggered following for TW and cars